

Replacing $\text{Ag}^{\text{TS}}\text{SCH}_2\text{-R}$ with $\text{Ag}^{\text{TS}}\text{O}_2\text{C-R}$ in EGaIn-Based Tunneling Junctions Does Not Significantly Change Rates of Charge Transport**

Kung-Ching Liao, Hyo Jae Yoon, Carleen M. Bowers, Felice C. Simeone, and George M. Whitesides*

Abstract: This paper compares rates of charge transport by tunneling across junctions with the structures $\text{Ag}^{\text{TS}}\text{X}-(\text{CH}_2)_n\text{CH}_3//\text{Ga}_2\text{O}_3/\text{EGaIn}$ ($n=1-8$ and $\text{X} = -\text{SCH}_2-$ and $-\text{O}_2\text{C}-$); here Ag^{TS} is template-stripped silver, and EGaIn is the eutectic alloy of gallium and indium. Its objective was to compare the tunneling decay coefficient (β , \AA^{-1}) and the injection current (J_0 , A cm^{-2}) of the junctions comprising SAMs of *n*-alkanethiolates and *n*-alkanoates. Replacing $\text{Ag}^{\text{TS}}\text{SCH}_2\text{-R}$ with $\text{Ag}^{\text{TS}}\text{O}_2\text{C-R}$ ($\text{R} = \text{alkyl chains}$) had no significant influence on J_0 (ca. $3 \times 10^3 \text{ A cm}^{-2}$) or β ($0.75-0.79 \text{ \AA}^{-1}$)—an indication that such changes (both structural and electronic) in the $\text{Ag}^{\text{TS}}\text{XR}$ interface do not influence the rate of charge transport. A comparison of junctions comprising oligo(phenylene)carboxylates and *n*-alkanoates showed, as expected, that β for aliphatic (0.79 \AA^{-1}) and aromatic (0.60 \AA^{-1}) SAMs differed significantly.

Studies of charge tunneling through self-assembled monolayer (SAM)-based junctions have focused predominately on the influence of backbone substituents^[1] or terminal functional groups^[2] on rates of charge transport. The effect of changing the group (which we call the “anchoring group”) that links the SAM to the metal substrate has not been explored in detail: only a few studies have examined this issue at the single-molecule level using scanning tunneling microscopy^[3] or conducting atomic force microscopy.^[4] Here, we examine the influence on tunneling current of changing the anchoring group from thiolate to carboxylate using a large-area ($50 \mu\text{m}^2$ of geometrical contact on average) SAM-based junction having the structure $\text{Ag}^{\text{TS}}\text{-X}-(\text{CH}_2)_n\text{CH}_3//\text{Ga}_2\text{O}_3/\text{EGaIn}$ ^[5] (where X is the anchoring group for the SAM; Ag^{TS}

is a template-stripped silver substrate.^[6] EGaIn is a liquid metal, eutectic gallium–indium alloy, and Ga_2O_3 is a thin semiconducting film that forms spontaneously on the surface of EGaIn in air.^[7] We prepared analogous junctions, compositionally different only in the replacement of $\text{Ag}^{\text{TS}}\text{SCH}_2\text{-R}$ with $\text{Ag}^{\text{TS}}\text{O}_2\text{C-R}$, and compared the rates of charge transport by tunneling through these two junctions. The similarity in these rates establishes that the rate of charge transport across the SAM-based tunneling junction is (perhaps surprisingly) insensitive to changes in the composition of the interface between the Ag^{TS} and the SAM.

While the study of organothiolates in molecular electronics is limited by the availability and stability of thiols, a very wide variety of carboxylic acids is commercially available, or easily accessible by straightforward synthetic routes. The ability to study charge transport through junctions of the structure $\text{Ag}^{\text{TS}}\text{O}_2\text{C-R}/\text{Ga}_2\text{O}_3/\text{EGaIn}$ makes mechanistic studies of tunneling much more accessible experimentally than it would be if only thiolates on Au or Ag could be studied. This research thus provides a new system that helps to clarify the role of the interfaces to electrodes in tunneling junctions based on SAMs.

The rate of charge transport by tunneling through SAMs decays exponentially with increasing distance between the top and bottom electrodes. In studies yielding results analogous to those from many other systems, we determined that junctions of the structure $\text{Ag}^{\text{TS}}\text{SCH}_2(\text{CH}_2)_n\text{CH}_3//\text{Ga}_2\text{O}_3/\text{EGaIn}$ (across a range of molecular lengths and structures) obey the simplified Simmons Equation (1),^[8] where J (A cm^{-2}) is the measured current density, and β (\AA^{-1}) is the tunneling decay coefficient.

$$J(V) = J_0(V) e^{-\beta d}. \quad (1)$$

We take d (\AA) to be the length of the molecule. The injection current, $J_0(V)$, represents the current density when $d=0$; that is, the value of $J(V)$ for a hypothetical system consisting only of the top and bottom electrodes, and the metal–SAM interfaces.^[5] Values of β that characterize tunneling junctions having a range of alkyl structures are similar; whereas values of $J_0(V)$ differ for different types of junctions, for reasons that are at least partially understood.^[5,9]

In an electrode–SAM–electrode junction, charge crosses a tunneling barrier whose energetic topography is not known exactly, but which describes the space (including the SAM, the interfaces between the SAMs and the electrodes, and any surface films on the electrodes) between the two metallic junctions. In principle, one approach to manipulating the shape of the tunneling barrier, and thus to influencing the rate

[*] Dr. K.-C. Liao, Dr. H. J. Yoon, Dr. C. M. Bowers, Dr. F. C. Simeone, Prof. Dr. G. M. Whitesides
 Department of Chemistry and Chemical Biology, Harvard University
 12 Oxford Street, Cambridge, MA 02138 (USA)
 E-mail: gwhitesides@gmwgroup.harvard.edu

Prof. Dr. G. M. Whitesides
 Wyss Institute for Biologically Inspired Engineering, Harvard University, 60 Oxford Street, Cambridge, MA 02138 (USA)
 and
 Kavli Institute for Bionano Science & Technology, Harvard University, 29 Oxford Street, Cambridge, MA 02138 (USA)

[**] This work was fully supported by a subcontract from Northwestern University from the Department of Energy (DE-SC0000989) on materials and measurements of charge transport. We thank Dr. Mathieu Gonidec and Dr. Jabulani R. Barber for their technical contributions.

Supporting information for this article is available on the WWW under <http://dx.doi.org/10.1002/anie.201308472>.

of charge transport, is to introduce functional groups into the structure of the SAM that are capable of influencing this topography, and thus the rate or mechanism of charge transport.^[1b,10] Using Ga₂O₃/EGaIn top-electrodes, however, we reported previously that the tunneling current is insensitive to the incorporation of several functional groups familiar in organic chemistry (e.g., an amide, –CONH– or –NHCO–) in the backbone of the molecules in the SAM,^[1e] or a variety of functional groups (both aliphatic and aromatic) that are not electrochemically active at the terminus of the SAM ostensibly in contact with the Ga₂O₃ film.^[2d]

Most studies using EGaIn-based tunneling junctions have focused on SAMs of *n*-alkanethiolates on Au or Ag. This focus on systems based on the Ag-SR anchoring group takes advantage of the extensive literature on these SAMs,^[11] but has limited our understanding of the role of the interface between the Ag (or Au) and the SAM to a single chemical and electronic structure. Here, we replaced *n*-alkanethiolates with *n*-alkanoates in order to examine the effect of the bottom-interface on the value of J_0 for a Ag^{TS}-SAM//Ga₂O₃/EGaIn junction. *n*-Alkanoic acids form highly ordered monolayers on metal surfaces;^[12] in particular, monolayers composed of long-chain *n*-alkanoates on Ag exhibit nearly crystalline packing of the hydrocarbon backbone, all-*trans* methylene conformations, and a bidentate ionic coordination of the carboxylate to the surface.^[12,13] Previous reports^[14] showed that the carboxylate moiety coordinates through ionic interactions with the surface of the Ag, and a native oxide of Ag possibly (or in our view probably) exists at the interface between the metal and the carboxylate. SAMs of *n*-alkanethiolates on Ag(111) have a ($\sqrt{7} \times \sqrt{7}$)R10.9° cell with 4.4 Å nearest neighbor spacing.^[15] The structure of *n*-alkanoate SAMs on Ag is comparable to that of *n*-alkanethiolates; the tilt angle of the alkyl chains is 15–25° (from the surface normal), and they form a *p*(2×2) overlayer with a lattice spacing of 5.8 Å, indicating a densely packed monolayer,^[14b] as summarized in Table S1 (see Supporting Information).

We prepared SAMs with commercially available *n*-alkanoic acids, HO₂C(CH₂)_{*n*}CH₃ where *n* = 1–8 (i.e., the number of methylene groups). The preparation of *n*-alkanoate SAMs on Ag^{TS} followed previously reported procedures.^[12] Freshly prepared Ag^{TS} substrates^[6] were introduced into a solution of 1 mM *n*-alkanoic acid in anhydrous *n*-hexadecane under N₂ for 3 h. After incubation at room temperature, we rinsed the SAM-bound Ag substrates three times with anhydrous hexane and dried the substrates under a gentle stream of nitrogen (see Supporting Information). We characterized the surface of SAMs of *n*-alkanoates on Ag^{TS} by using contact angle measurements. The monolayers exhibited low wettability: static contact angles for wetting by water and *n*-hexadecane were 113 ± 7° and 45 ± 3°, respectively. These values are consistent with previous reports by Tao et al.^[12] and Lin et al.^[13]

We measured $J(V)$ for junctions of the form Ag^{TS}O₂C(CH₂)_{*n*}CH₃//Ga₂O₃/EGaIn over the range of ±0.5 V as a function of the length of alkyl chain (*n* = 1–8); we did not observe rectification of current (Figure 1b). We compared the values of $\log |J(-0.5 \text{ V})|$; each curve of $\log |J(V)|$ versus V was generated with 430–720 data from at least 20 different

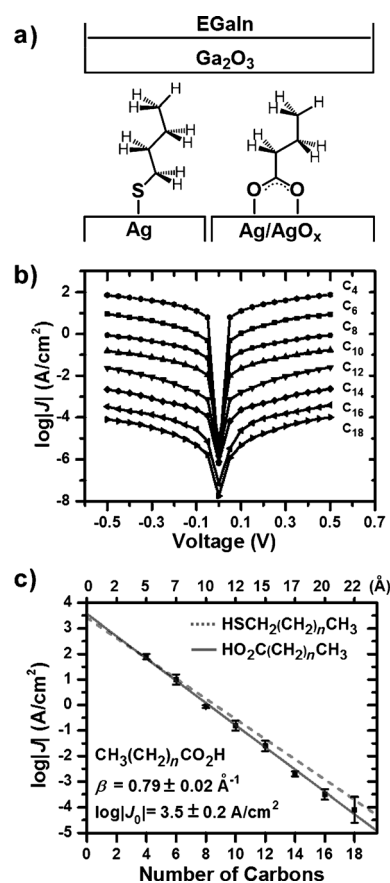


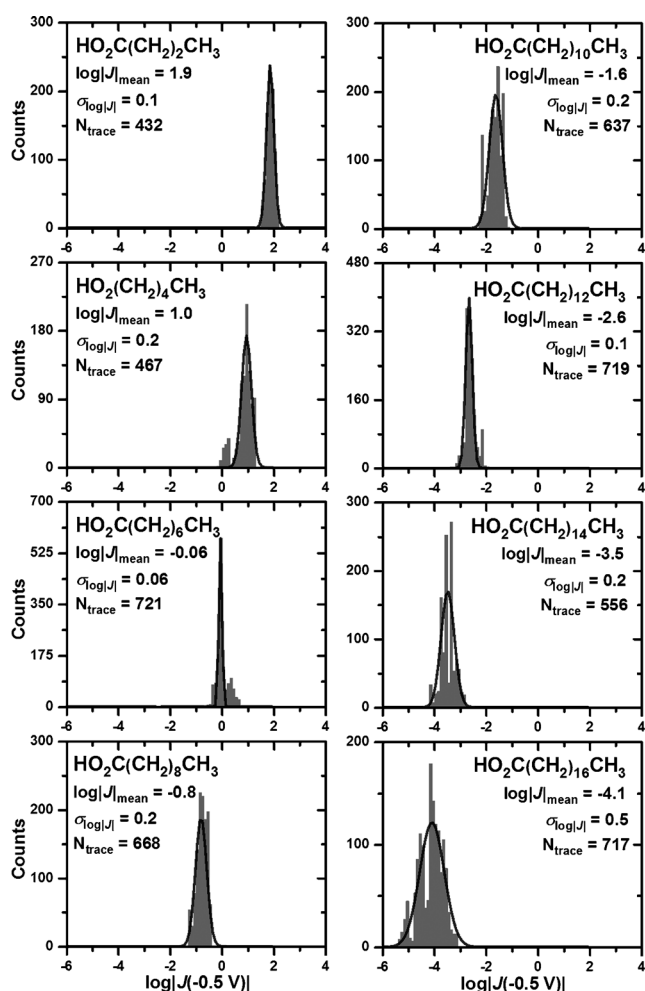
Figure 1. a) A cartoon representation of the Ag^{TS}X_R/Ga₂O₃/EGaIn junction (X = –SCH₂– and –O₂C–); b) log current density ($\log |J|$) versus bias (V) plots for the Ag^{TS}O₂C(CH₂)_{*n*}CH₃//Ga₂O₃/EGaIn junctions with various chain lengths (4–18 carbons including the top methyl group and the bottom anchoring group), as indicated in the figure; c) a plot of log current density ($\log |J|$) against the chain length of *n*-alkanoates (including the terminal C–H bond), given in number of carbons at –0.5 V. The linear-least square fits for *n*-alkanoates (dotted line) and for *n*-alkanethiolates (solid line) and the results of electrical measurements are inserted in the figure.

junctions on three to four samples, and the yield of working junctions was ≥ 84 % (Table 1). As observed in many previous studies,^[9,16] the binned J values (100 bins in the range of $\log |J| = -6$ to 4, with units of A cm⁻²; the width of each bin is $\log |J| \approx 0.1$) had a distribution that was approximately log-normal; this form justified fitting each histogram of $\log |J|$ with a Gaussian curve. From these fittings, we obtained mean values of $\log |J|$ ($\log |J|_{\text{mean}}$) and standard deviations (σ_{\log}) of the corresponding Gaussian fits (Figure 2); $\log |J|_{\text{mean}}$ is indistinguishable from the log median value ($\log |J|_{\text{median}}$) of $\log |J|$ determined in each histogram (Table 1). Values of σ_{\log} ranged from 0.1 to 0.5; these values are similar to those observed in the junctions of *n*-alkanethiolate SAMs.^[5] As expected from the simplified Simmons equation, the rate of charge transport across junctions containing SAMs of *n*-alkanoates followed an exponential decrease with increasing length of the *n*-alkyl groups (*n* = 1–8 for O₂C(CH₂)_{*n*}CH₃). Figure 1c shows a plot of $\log |J|$ versus calculated length (Å) which includes the length of terminal H–C bond but excludes

Table 1: Summary of the data derived from *n*-alkanoates (C_{*n*}O₂) and *n*-alkanethiolates (C_{*n*}S) at −0.5 V to illustrate the similarity in the charge transport characteristics among the two homologous SAMs.

C _{<i>n</i>} O ₂	<i>n</i> -Alkanoates						<i>n</i> -Alkanethiolates	
	Number of Samples	Working Junctions	Yield [%]	Traces	log <i>J</i> _{median} [A cm ^{−2}]	log <i>J</i> _{mean} ± σ _{log} [A cm ^{−2}]	C _{<i>n</i>} S	log <i>J</i> _{mean} ± σ _{log} [A cm ^{−2}]
C ₄ O ₂	3	20	95	432	1.85	1.9 ± 0.1	C ₄ S	1.6 ± 0.5
C ₆ O ₂	3	20	90	467	0.95	1.0 ± 0.2	C ₆ S	0.9 ± 0.3
C ₈ O ₂	4	30	97	721	−0.05	−0.06 ± 0.06	C ₈ S	0.2 ± 0.3
C ₁₀ O ₂	4	29	91	668	−0.85	−0.8 ± 0.2	C ₁₀ S	−1.1 ± 0.3
C ₁₂ O ₂	3	27	90	637	−1.65	−1.6 ± 0.2	C ₁₂ S	−1.5 ± 0.5
C ₁₄ O ₂	4	32	97	719	−2.65	−2.7 ± 0.1	C ₁₄ S	−2.2 ± 0.3
C ₁₆ O ₂	3	24	91	556	−3.55	−3.5 ± 0.2	C ₁₆ S	−3.2 ± 0.3
C ₁₈ O ₂	4	32	84	717	−4.15	−4.1 ± 0.5	C ₁₈ S	−3.9 ± 0.3
log <i>J</i>₀ 						3.5 ± 0.2	log <i>J</i>₀ 	
β = 0.79 ± 0.02 Å^{−1} (1.00 ± 0.02 n_c^{−1})							3.4 ± 0.3	
							β = 0.75 ± 0.02 Å^{−1}	

the length of Ag–O bond, which we considered to be a part of the Ag^{TS}–SAM interface. In this view, [S]CH₂(CH₂)_{2*n*}CH₃ and [O₂]C(CH₂)_{2*n*}CH₃ are comparable structures in terms of the


Figure 2. Histograms for values of log |*J*| data derived from *n*-alkanoates at −0.5 V (each trace generates two data points from the forward and reverse bias; we describe the junction measurement protocol in more detail in the Supporting Information). Each histogram is fitted with a Gaussian curve (black curve).

dimensions of the tunneling barrier they provide. The linear-least square fit of the full set of data (HO₂C(CH₂)_{2*n*}CH₃, *n* = 1–8) yielded the log-injection current, log |*J*₀| = 3.5 ± 0.2 A cm^{−2} at (coefficient of determination, *R*² = 0.99). The slope derived from the plot of ln |*J*| versus the length of molecules provided the tunneling decay coefficient, β = 0.79 ± 0.02 Å^{−1}.

Comparisons of *J*(*V*) data from *n*-alkanethiolate^[5] and *n*-alkanoate SAMs on Ag/Ag(O_{*x*}) (Table 1) indicate that these junctions have a indistinguishable tunneling decay coefficient (β = 0.79 ± 0.02 Å^{−1} for *n*-alkanoates; β = 0.75 ± 0.02 Å^{−1} for *n*-alkanethiolates, both with even numbers of carbon atoms) and injection current (log |*J*₀| = 3.5 ± 0.2 A cm^{−2} derived from *n*-alkanoates; log |*J*₀| = 3.4 ± 0.3 A cm^{−2} derived from *n*-alkanethiolates). The similarities in β and *J*₀ imply that any difference in the contribution of the Ag–thiolate and the Ag–oxygen interface to the shape of the tunneling barrier is not detectable by our methods, although these two interfaces are chemically and electronically quite different. We conclude therefore, that the Ag^{TS}–X–R interface does not contribute to the features of the tunneling barrier that influence tunneling current. We note that a layer of AgO_{*x*} probably exists at the interface between the Ag metal and the alkanoate SAM; this layer is not present at the Ag–thiolate interface.^[17] While we and Tao et al. have not yet defined whether mono- or multilayers of native silver oxide are sandwiched between the Ag metal and the carboxylate, the *J*–*V* measurements suggest that this film, if any, is sufficiently conductive that it makes no contribution to the resistance of the junction. Levine et al. reported a similar observation in examining the electrical properties of AlO_{*x*} in Al–AlO_{*x*}/alkyl-phosphonate//Hg junctions.^[18]

Several studies have predicted or reported a distinct electronic influence from different metal–molecule interfaces used in junction measurements.^[3a,19] For example, Zimbovskaya and Pederson^[20] examined different metal–molecule interfaces theoretically, and concluded that different modes of binding at the interfaces might influence the conductance of junctions. In large-area (submicro- to micrometer area) junctions, Chu et al.^[21] reported that the current through molecules with an Au–amine junction is larger by a factor of 10 than that with an Au–thiolate linkage, and attributed this observation to differences in the electronic interactions between the gold and the anchoring group. Several studies of single-molecule or nanometer-scale junction have concluded similarly that the anchoring group of the molecule influences the rate of charge transport (up to an order of magnitude).^[3a,4b,19] Our findings, however, indicate that replacing AgSCH₂–R with AgO₂C–R (a large change in the structure of the bottom metal–SAM interface) has no significant influence (less than a factor of two) on the rates of charge transport across *n*-alkyl-based SAMs.

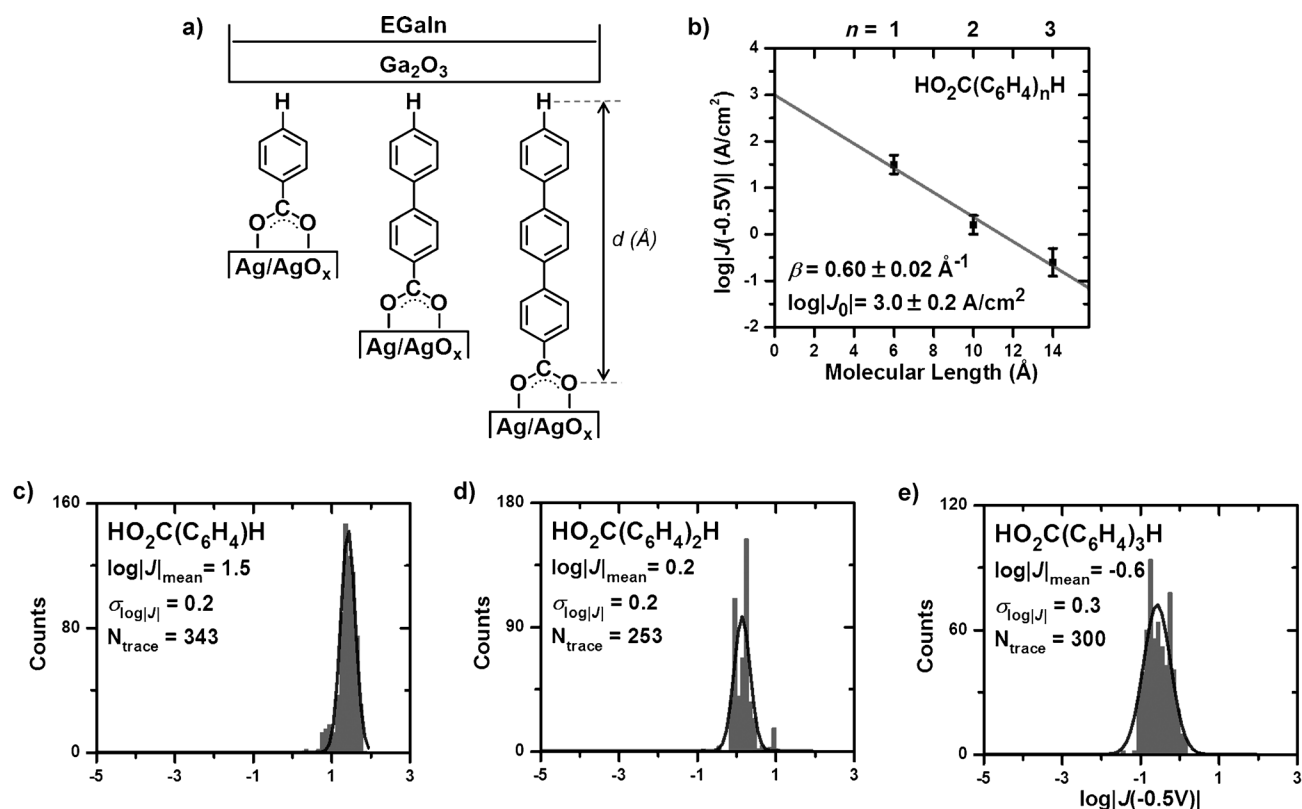


Figure 3. a) A cartoon representation of the junction structure comprising oligo(phenylene)-carboxylate SAMs. The carboxylate forms a bidentate coordination to the surface of Ag. The length of molecule (d) is measured from the bottom oxygen to the distal hydrogen; b) a plot of $\log |J|$ against the length of molecule (in Å), including the terminal C–H bond, of oligo(phenylene)carboxylates, given in the number of phenylene units at -0.5 V. The linear-least square fits (solid line) and the results of electrical measurement are inserted in the figure. Histograms of $\log |J|$ for c) benzoate; d) biphenyl-4-carboxylate; and e) *p*-terphenyl-4-carboxylate in the $\text{Ag}^{\text{TS}}\text{O}_2\text{C}(\text{C}_6\text{H}_4)_n\text{H}/\text{Ga}_2\text{O}_3/\text{EGaIn}$ junctions ($n=1-3$) at -0.5 V. Each histogram is fitted with a Gaussian curve (black curve).

Tao and coworkers reported the formation and characterization of SAMs of biphenyl-4-carboxylic acid^[22] and *p*-terphenyl-4-carboxylic acid^[14b] on Ag. Their report showed that the oligo(phenylene)carboxylate binds perpendicularly to the surface through a symmetric ionic coordination to the surface of Ag.^[22] We incorporated SAMs of oligo(phenylene)-carboxylic acids into junctions of the structure $\text{Ag}^{\text{TS}}\text{O}_2\text{C}(\text{C}_6\text{H}_4)_n\text{H}/\text{Ga}_2\text{O}_3/\text{EGaIn}$ ($n=1-3$) and characterized rates of charge transport across them (Figure 3a; Table 2). We did not observe a significant rectification of current at ± 1.0 V (Figure S1). Figure 3c–e show the histograms of $\log |J|$ at -0.5 V for benzoic acid, biphenyl-4-carboxylic acid, and *p*-

terphenyl-4-carboxylic acid. We found a narrow distribution of current density with a small range of σ_{\log} (0.2–0.3) for each SAM. We estimated the value of $\log |J_0|$ ($3.0 \pm 0.2 \text{ A cm}^{-2}$) of the $\text{Ag}^{\text{TS}}\text{O}_2\text{C}(\text{C}_6\text{H}_4)_n\text{H}/\text{Ga}_2\text{O}_3/\text{EGaIn}$ junctions from a linear least squares fit ($R^2=0.98$) of the plot of $\log |J|$ versus the calculated length of the molecules (Å); β was $0.60 \pm 0.02 \text{ Å}^{-1}$.

The tunneling decay coefficient of *n*-alkanoate-based SAMs (0.79 Å^{-1}) is higher than that of oligophenylene-containing SAM (0.60 Å^{-1}), and indicates (as have other studies)^[23] that in these oligophenylene-based SAMs 1) the shape of the tunneling barrier is influenced both by the width of the tunneling barrier and the electronic structure of the molecules forming the SAM; 2) charge transport by tunneling through poly-aromatic SAMs is more rapid than through non-conjugated SAMs of the same thickness. The value of $\log |J_0|$ derived from the junctions comprising SAMs of oligophenylene carboxylates ($\log |J_0| = 3.0 \pm 0.2 \text{ A cm}^{-2}$) is indistinguishable to that of *n*-alkanoates ($\log |J_0| = 3.5 \pm 0.2 \text{ A cm}^{-2}$) at the precision of our measurements.

Within the limits of accuracy and uncertainty in our system, the changes in the structure of the Ag–SAM interface we have examined have no statistically significant influence on the rates of tunneling across an *n*-alkane-based tunneling barrier, since the tunneling currents through junctions of *n*-alkanoate and of *n*-alkanethiolate SAMs are indistinguish-

Table 2: Summary of the data derived from oligo(phenylene)carboxylates ($\text{Ag}^{\text{TS}}\text{O}_2\text{C}(\text{C}_6\text{H}_4)_n\text{H}/\text{Ga}_2\text{O}_3/\text{EGaIn}$, $n=1-3$) at -0.5 V.

n	Oligo(phenylene)carboxylates					$\log J _{\text{median}}$ [A cm^{-2}]	$\log J _{\text{mean}} \pm \sigma_{\log}$ [A cm^{-2}]
	Number of Samples	Working Junctions	Yield [%]	Traces			
1	3	18	72	343	1.45	1.5 ± 0.2	
2	3	12	80	253	0.15	0.2 ± 0.2	
3	3	15	79	300	-0.55	-0.6 ± 0.3	

$\log |J_0|$
 $\beta = 0.60 \pm 0.03 \text{ Å}^{-1}$ ($2.4 \pm 0.1 n_{\text{C}_6\text{H}_4}^{-1}$) **3.0 ± 0.2**

able in our experiments. The details of the bonds at the $\text{Ag}^{\text{TS}}\text{O}_2\text{C-R}$ interface are quite different from those at the $\text{Ag}^{\text{TS}}\text{SCH}_2\text{-R}$ interface,^[14] and this study thus suggests that nature of the coordination between the metal of bottom electrode (Ag^{TS}) and the SAM does not significantly influence the rate of tunneling (at least in the two sets of compounds examined here). The tunneling decay coefficient for *n*-alkanoates and for *n*-alkanethiolates on silver are indistinguishable ($0.75\text{--}0.79 \text{ \AA}^{-1}$), and are similar to previous literature reports for junctions with different electrodes.^[5,9,18,24] The tunneling decay coefficient for oligophenylene carboxylates ($\beta = 0.60 \text{ \AA}^{-1}$) is, as expected from prior work,^[23a] significantly smaller than that of alkyl-based SAMs.

The $\text{Ag}^{\text{TS}}\text{O}_2\text{C-R//Ga}_2\text{O}_3/\text{EGaIn}$ junction emerges from this work as a versatile and convenient experimental system with which to investigate factors that influence rates of charge transport through SAM-based junctions, and to understand the mechanisms underlying these influences. The use of carboxylate anchoring groups promises to simplify the study of tunneling junctions greatly by eliminating the instability (due to oxidation, desulfurization, and other processes) and multiple chemical incompatibilities of the commonly studied structures based on organic thiolates. Moreover, carboxylates are more convenient than thiols in physical-organic studies, because they are commercially available, stable (especially to oxidation), and easily handled and purified. The data in this paper suggest—at least for junctions with high tunneling barriers—that Ag–SAM interfaces having either a thiolate or carboxylate anchoring group may be directly comparable.

Received: September 28, 2013

Revised: December 16, 2013

Published online: March 5, 2014

Keywords: alkanooates · charge transport · EGaIn junction · molecular electronics · self-assembled monolayer · tunneling

- [1] a) D. J. Wold, R. Haag, M. A. Rampi, C. D. Frisbie, *J. Phys. Chem. B* **2002**, *106*, 2813–2816; b) A. Salomon, D. Cahen, S. Lindsay, J. Tomfohr, V. B. Engelkes, C. D. Frisbie, *Adv. Mater.* **2003**, *15*, 1881–1890; c) R. L. McCreery, A. J. Bergren, *Adv. Mater.* **2009**, *21*, 4303–4322; d) D. Fracasso, H. Valkenier, J. C. Hummelen, G. C. Solomon, R. C. Chiechi, *J. Am. Chem. Soc.* **2011**, *133*, 9556–9563; e) M. M. Thuo, W. F. Reus, F. C. Simeone, C. Kim, M. D. Schulz, H. J. Yoon, G. M. Whitesides, *J. Am. Chem. Soc.* **2012**, *134*, 10876–10884.
- [2] a) R. L. McCreery, *Chem. Mater.* **2004**, *16*, 4477–4496; b) V. B. Engelkes, J. M. Beebe, C. D. Frisbie, *J. Am. Chem. Soc.* **2004**, *126*, 14287–14296; c) C. A. Nijhuis, W. F. Reus, G. M. Whitesides, *J. Am. Chem. Soc.* **2009**, *131*, 17814–17827; d) H. J. Yoon, N. D. Shapiro, K. M. Park, M. M. Thuo, S. Soh, G. M. Whitesides, *Angew. Chem.* **2012**, *124*, 4736–4739; *Angew. Chem. Int. Ed.* **2012**, *51*, 4658–4661.
- [3] a) F. Chen, X. Li, J. Hihath, Z. Huang, N. Tao, *J. Am. Chem. Soc.* **2006**, *128*, 15874–15881; b) Y. S. Park, A. C. Whalley, M. Kamenetska, M. L. Steigerwald, M. S. Hybertsen, C. Nuckolls, L. Venkataraman, *J. Am. Chem. Soc.* **2007**, *129*, 15768–15769; c) Z. Li, M. Smeu, M. A. Ratner, E. Borguet, *J. Phys. Chem. C* **2013**, *117*, 14890–14898.
- [4] a) J. M. Beebe, V. B. Engelkes, L. L. Miller, C. D. Frisbie, *J. Am. Chem. Soc.* **2002**, *124*, 11268–11269; b) B. Kim, J. M. Beebe, Y. Jun, X. Y. Zhu, C. D. Frisbie, *J. Am. Chem. Soc.* **2006**, *128*, 4970–4971; c) S. Ahn, S. V. Aradhya, R. S. Klausen, B. Capozzi, X. Roy, M. L. Steigerwald, C. Nuckolls, L. Venkataraman, *Phys. Chem. Chem. Phys.* **2012**, *14*, 13841–13845.
- [5] F. C. Simeone, H. J. Yoon, M. M. Thuo, J. R. Barber, B. Smith, G. M. Whitesides, *J. Am. Chem. Soc.* **2013**, *135*, 18131–18144.
- [6] E. A. Weiss, G. K. Kaufman, J. K. Kriebel, Z. Li, R. Schalek, G. M. Whitesides, *Langmuir* **2007**, *23*, 9686–9694.
- [7] R. C. Chiechi, E. A. Weiss, M. D. Dickey, G. M. Whitesides, *Angew. Chem.* **2008**, *120*, 148–150; *Angew. Chem. Int. Ed.* **2008**, *47*, 142–144.
- [8] a) J. G. Simmons, *J. Appl. Phys.* **1963**, *34*, 1793–1803; b) J. G. Simmons, *J. Appl. Phys.* **1963**, *34*, 2581–2590.
- [9] C. A. Nijhuis, W. F. Reus, J. R. Barber, G. M. Whitesides, *J. Phys. Chem. C* **2012**, *116*, 14139–14150.
- [10] S. V. Aradhya, L. Venkataraman, *Nat. Nanotechnol.* **2013**, *8*, 399–410.
- [11] J. C. Love, L. A. Estroff, J. K. Kriebel, R. G. Nuzzo, G. M. Whitesides, *Chem. Rev.* **2005**, *105*, 1103–1170.
- [12] Y. T. Tao, *J. Am. Chem. Soc.* **1993**, *115*, 4350–4358.
- [13] S.-Y. Lin, T.-K. Tsai, C.-M. Lin, C.-h. Chen, Y.-C. Chan, H.-W. Chen, *Langmuir* **2002**, *18*, 5473–5478.
- [14] a) Y.-T. Tao, G. D. Hietpas, D. L. Allara, *J. Am. Chem. Soc.* **1996**, *118*, 6724–6735; b) M.-H. Hsu, W.-S. Hu, J.-J. Lin, Y.-J. Hsu, D.-H. Wei, C.-W. Yang, C.-S. Chang, Y.-T. Tao, *Langmuir* **2004**, *20*, 3641–3647.
- [15] M. Kawasaki, M. Iino, *J. Phys. Chem. B* **2006**, *110*, 21124–21130.
- [16] W. F. Reus, C. A. Nijhuis, J. R. Barber, M. M. Thuo, S. Tricard, G. M. Whitesides, *J. Phys. Chem. C* **2012**, *116*, 6714–6733.
- [17] M. Himmelhaus, I. Gauss, M. Buck, F. Eisert, C. Wöll, M. Grunze, *J. Electron Spectrosc. Relat. Phenom.* **1998**, *92*, 139–149.
- [18] I. Levine, S. M. Weber, Y. Feldman, T. Bendikov, H. Cohen, D. Cahen, A. Vilan, *Langmuir* **2012**, *28*, 404–415.
- [19] W. Hong, D. Z. Manrique, P. Moreno-García, M. Gulcur, A. Mishchenko, C. J. Lambert, M. R. Bryce, T. Wandlowski, *J. Am. Chem. Soc.* **2012**, *134*, 2292–2304.
- [20] N. A. Zimbovskaya, M. R. Pederson, *Phys. Rep.* **2011**, *509*, 1–87.
- [21] C. Chu, J.-S. Na, G. N. Parsons, *J. Am. Chem. Soc.* **2007**, *129*, 2287–2296.
- [22] Y. T. Tao, M. T. Lee, S. C. Chang, *J. Am. Chem. Soc.* **1993**, *115*, 9547–9555.
- [23] a) R. E. Holmlin, R. Haag, M. L. Chabiny, R. F. Ismagilov, A. E. Cohen, A. Terfort, M. A. Rampi, G. M. Whitesides, *J. Am. Chem. Soc.* **2001**, *123*, 5075–5085; b) D. Fracasso, M. I. Muglali, M. Rohwerder, A. Terfort, R. C. Chiechi, *J. Phys. Chem. C* **2013**, *117*, 11367–11376.
- [24] A. Salomon, H. Shpaisman, O. Seitz, T. Boecking, D. Cahen, *J. Phys. Chem. C* **2008**, *112*, 3969–3974.